6110-232:JKR

1. AGENCY USE ONLY (Leave blank)	2. REPORT DATE	3. REPORT TYPE AND DATES COVERED
	5/29/92	12/31/92 Technical Report

4. TITLE AND SUBTITLE: Probing Thin-Film $YBa_2Cu_3O_{7-\delta}$ Superconductors by Second Harmonic Generation Using Femtosecond Laser Pulses

5. FUNDING NUMBERS
C: N0001491WX24208
PE: 61153N-13
PR: RR013-10-0G and RR013-08-0C
TA: 413r011---01
WU: 61-3732-00

6. AUTHOR(S)
Jane K. Rice, S.W. McCauley[a], A.P. Baronavski, J.S. Horwitz and D.B. Chrisey

7. PERFORMING ORGANIZATION NAME(S) AND ADDRESS(ES)
Naval Research Laboratory
Washington, DC 20375-5000
(Code 6111, J.K. Rice)

8. PERFORMING ORGANIZATION REPORT NUMBER
Technical Report #1

9. SPONSORING/MONITORING AGENCY NAME(S) AND ADDRESS(ES)
Office of Naval Research
800 North Quincy Street
Arlington, VA 22217-5000

10. SPONSORING/MONITORING AGENCY REPORT NUMBER
Technical Report #1

11. SUPPLEMENTARY NOTES
[a]Physics Department, California State Polytechnic University, Pomona, CA

12a. DISTRIBUTION/AVAILABILITY STATEMENT
This document has been approved for public release and sale, distribution of this document is unlimited.

13. ABSTRACT (Maximum 200 words)

High temperature superconducting thin films of $YBa_2Cu_3O_{7-\delta}$ are examined by measuring the second-harmonic-generated (SHG) signal from an incident 60 fs laser pulse of 2.0 eV (620 nm) in air at room temperature. As oxygen stoichiometry is varied ($0.00 < \delta < 0.50$), large changes in the SHG intensity are observed. The oxygen content of the films is independently determined by measuring *i)* the c-axis lattice parameter derived from x-ray diffraction and *ii)* the stoichiometry of the films determined by elastic backscattering spectrometry. We report a negative correlation of the SHG intensity with the c-axis parameter indicating that a known compression of the c-axis leads to a *larger* SHG signal. An additional experiment in which the SHG intensity is monitored as a function of temperature (300 K to 20 K) in vacuum is performed. A gradual increase of $\sim 50\%$ in the SHG intensity is observed as the temperature is lowered which can also be correlated to a decrease in the length of the c-axis. Other experiments including rotation anisotropy and polarization of the incident and analyzer beams are also discussed.

Ultrafast Phenomena, thin films, second harmonic generation, superconductors

Unclassified | Unclassified | Unclassified

OFFICE OF NAVAL RESEARCH

GRANT or CONTRACT N0001491WX24208

R&T Code 413r011 --- 01

Technical Report No. 1

Probing Thin-Film $YBa_2Cu_3O_{7-\delta}$ Superconductors by Second Harmonic Generation using Femtosecond Laser Pulses

Jane K. Rice, S.W. McCauley[a] and A.P. Baronavski
Naval Research Laboratory
Chemistry Division, Code 6111
Washington, DC 20375-5000

and

J.S. Horwitz and D.B. Chrisey
Naval Research Laboratory
Condensed Matter and Radiation Sciences Division, Code 4673
Washington, DC 20375-5000

[a]Permanent Address: Physics Department, California State Polytechnic University, Pomona, CA 91768

To be submitted to:
The Journal of Applied Physics,
June 1992.

Probing Thin-film $YBa_2Cu_3O_{7-\delta}$ Superconductors by Second Harmonic Generation using Femtosecond Laser Pulses

Jane K. Rice, S. W. McCauley[a] and A.P. Baronovski
Chemistry Division, Code 6111

and

J.S. Horwitz and D.B. Chrisey
Condensed Matter and Radiation Sciences Division, Code 4673
Naval Research Laboratory, Washington, D.C. 20375-5000

[a] Permanent Address: Physics Department, California State Polytechnic University, Pomona, CA 91768

Submitted to:
Physical Review B,
June 1992.

Abstract

High temperature superconducting thin films of $YBa_2Cu_3O_{7-\delta}$ are examined by measuring the second-harmonic-generated (SHG) signal from an incident 60 fs laser pulse of 2.0 eV (620 nm) in air at room temperature. As oxygen stoichiometry is varied ($0.00 < \delta < 0.50$), large changes in the SHG intensity are observed. The oxygen content of the films is independently determined by measuring *i)* the c-axis lattice parameter derived from x-ray diffraction and *ii)* the stoichiometry of the films determined by elastic backscattering spectrometry. We report a negative correlation of the SHG intensity with the c-axis parameter indicating that a known compression of the c-axis leads to a *larger* SHG signal. An additional experiment in which the SHG intensity is monitored as a function of temperature (300 K to 20 K) in vacuum is performed. A gradual increase of $\sim 50\%$ in the SHG intensity is observed as the temperature is lowered which can also be correlated to a decrease in the length of the c-axis. Other experiments including rotation anisotropy and polarization of the incident and analyzer beams are also discussed.

INTRODUCTION:

Second harmonic generation (SHG) from surfaces has proven to be a highly informative probe of interfacial boundaries. Initial studies of the nonlinear response from a metal surface have been followed by the application of SHG to gain information concerning molecular orientation, concentration, and species identification on surfaces.[1-3]. One of the problems in these studies has been damage to the surface under study. The damage results from the high peak powers ($>$ 10 MW/cm^2) necessary to obtain reasonable signals. For nanosecond lasers, this power corresponds to $>$ 10 mJ/cm^2, which is enough to cause local melting of the surface or, at the very least, disruption of the more labile bonds. For this reason, femtosecond lasers possess a real advantage over other laser sources. Their short pulse widths ($\sim 100 \times 10^{-15}$ s) mean intensities of 10 MW/cm^2 can easily be attained with corresponding fluences of only 10 μJ/cm^2. Therefore, surface damage can be eliminated entirely in most cases and several surface characteristics can be probed.

We address two important aspects of surface diagnostic experiments on thin-film high temperature superconductors (HTSC). First, the use of femtosecond pulses to produce SHG can provide a *non-intrusive* and *non-destructive* means of probing these materials.[1,3] Second, since the first technological application of HTSC materials has been as thin-films, a technique which has the potential to monitor the chemical structure or free electron density near the surface (within $\sim$500 Å) is extremely desirable. SHG from several HTSC materials has been reported in which absolute intensities of SHG and third harmonic generation (THG) have been examined.[4]

They also report a relative intense SHG signal from YBCO compared to silicon.[4] Others have reported SHG from the $La_{1.8}Sr_{0.2}CuO_4$ superconductor.[5]

An example of the need for further SHG studies is demonstrated by the importance of understanding the dependence of SHG on oxygen deficiencies in the crystal lattice, particularly the deficiencies of oxygen atoms near the film surface. It is known that the highest critical temperatures (T_c's) for these films are attained only for a specific stoichiometry of oxygen.[6-8] A compositional change from $\delta = 1$ to 0 for $YBa_2Cu_3O_{7-\delta}$ (YBCO) is known to effect the crystal structure, e.g., lattice parameters of the film and yield a variation in the electrical properties from insulating to superconducting. Many aspects of the influence of the structural parameters on the electrical properties are still not well understood.

The origin of SHG from a metal surface is due to the dipole term of the susceptibility, which is non-zero at the interface of a centrosymmetric material.[1-3] This is defined as a material in which an inversion through the center of the unit cell leads to an identical species. A bulk term, originating from magnetic dipole terms[9], may also contribute to the SHG. The intensity of the reflected SHG from excitation by a plane wave of frequency ω and polarization $\mathbf{e}(\omega)$ is

$$I(2\omega) = \frac{32\pi^3\omega^2\sec^2\theta_{2\omega}}{c^3\epsilon_1(\omega)\epsilon_1^{1/2}(2\omega)} \left| \mathbf{e}(2\omega)\cdot\chi^{(2)}_{s,eff}:\mathbf{e}(\omega)\mathbf{e}(\omega) \right|^2 I^2(\omega) \qquad (1)$$

where $\theta_{2\omega}$ is the angle of incidence relative to the surface normal and I(ω) is the pump intensity. The symbols, e(ω) and e(2ω) are related to the unit polarization vectors by the Fresnel coefficients. The nonlinear susceptibility, $\chi^{(2)}_{s,eff}$ at the surface includes surface $\chi^{(2)}_{s,eff}$ and bulk magnetic dipole contributions. The tensor, $\chi^{(2)}_{s,eff}$ simplifies to 3 non-zero elements for an isotropic medium.

The YBCO crystal structure is centrosymmetric. The thin-films used in this study have near-single-crystal structure and are centrosymmetric. They have no electrostatic bulk term, except those generated from possible defects in the film. Since $p_{(out)}$ polarization contains contributions from all the $\chi^{(2)}_{s,eff}$ elements, surface and bulk effects cannot be separated.[2] In YBCO, magnetic terms are small, therefore, the SHG intensity is expected to originate from the surface term. The SHG component due to the surface current can be classified as parallel or perpendicular to the surface.[3] In the geometry used here the p output of SHG is examined, addressing the current flow perpendicular to surface. Examination of the origin of the SHG dependence reported here can provide a way to monitoring changes in the surface of the thin films, at the least, and may help in determining the parameters important to the superconducting state.

EXPERIMENTAL:

The experiments reported here were carried out in three stages. At first, preliminary SHG measurements were made on several YBCO films. The film thicknesses varied from 400 to 6000 Å, they were deposited on MgO<100> or $SrTiO_3$ <100> substrates and had T_c's of

~84 K. In addition, one oxygen deficient film (T_c= 57 K) was examined and indicated a much lower SHG intensity than films of T_c ~84 K. This was followed by a pilot study of four films made under controlled conditions and characterized for film structure by x-ray diffraction(XRD), atomic composition by elastic backscattering spectrometry(EBS) and DC transport indicated by T_c and J_c @77 K. These characterizations were followed by the SHG and reflection measurements. Two of the films had a T_c~90K which we will refer to as "normal" (labeled N1 and N6) and two were oxygen deficient films (labeled D1 and D6). One pair of normal and oxygen deficient films were grown on the MgO<100> substrate and the other on $SrTiO_3$<100>. The same SHG intensity dependence on the oxygen content was observed. Thirteen additional films, eight on MgO and five on $SrTiO_3$, six of 6000 Å thickness, and seven oxygen deficient were added to the study. These were made six months after the four pilot films with the exception of D9, which was made nine months later. Characterization of these films (including EBS on $SrTiO_3$ substrates) was done after the SHG measurements were completed. This accounts for the 17 films which provide the statistical basis for the film parameters and SHG correlations presented here.

A) Film Preparation.

The YBCO films were prepared by pulsed laser deposition.[10] The output of an EMG-315 KrF excimer laser operated at 248 nm with an energy of 125 mJ per pulse was focused to an energy density of ~2 J/cm^2 onto a rotating target of bulk superconducting material. The vaporized material was deposited onto a heated substrate (750°C) positioned 3 cm from the target. Films were typically deposited in a high background of O_2 (300 mTorr). Following

deposition, films were cooled in 1 atmosphere of O_2 to yield normal YBCO films (T_c = 90 K) or films were cooled in 300 mTorr of O_2 to yield oxygen deficient films with $T_c \sim 60$ K.[11]

Characterization of the films was carried out using standard techniques. Transition temperatures were determined from magnetic AC susceptibility measurements.[12] Films were characterized by XRD in the standard $\theta/2\theta$ mode using Cu(K_α) radiation. The c-axis lattice parameter was calculated from the 00,10 reflection. These XRD studies indicate that the YBCO films are oriented with the c-axis normal to the substrate and with the exception of film number D9, display narrow rocking curve widths of $0.15 < \Gamma < 0.28$ (for the 002 reflection). The lower limit for Γ of 0.15 represents the experimental resolution of the instrument. Oxygen stoichiometry and film thicknesses are measured using EBS with 6.2 Mev He^{+2} for those films deposited on $SrTiO_3$. Other film thicknesses are estimated from the deposition time.

B) Optical Measurements.

The laser apparatus used to make the SHG measurements at room temperature in air consisted of a femtosecond laser with pulses of ~ 60 fs duration and 4.5μJ/pulse, a sample mounting station, a monochromator and a photon counting system. The femtosecond laser pulses were produced by a colliding pulse mode-locked (CPM) laser (Clark, Inc.) which was amplified by a 350 Hz Lambda Physik (LPX-240i) excimer laser operating at 351 nm with 10 mJ of energy pumping a modified bow-tie amplifier (Clark,Inc). The output of the laser was horizontally polarized. The laser impinged on vertically mounted films on a rotating stage which was placed at a 45° angle to the incident beam. The reflected beam passed through a

polarization analyzer and several glass filters (UG-11 and 7-54), which transmitted the second harmonic at 310 nm and blocked the fundamental at 620 nm, onto the open slits of a 1/4 m Jarrell-Ash monochromator. A PMT(1P28) was used for light detection and the SHG signal is monitored by a photon counter (Stanford Research Systems 9400). For most of the results presented, multiple photon events were counted by scanning the discriminator value in 3.2mv increments. The threshhold value of 3.2 was determined by a test of the PMT output distribution as a function of discriminator voltage. The number of counts at the first discriminator value of 3.2mv represents a single count of all events whether they are single or multiple photon events. The discriminator voltage was then increased to 6.4 mv and the counts here represent the number of events generated from two simultaneous photons. The discriminator value was increased in 3.2 mv increments until the total number of counts (sum of all counts at all previous discriminator voltages) at that voltage was $< 2\%$ of the value at the lowest (3.2 mv) discriminator voltage. Multiple photon events were counted in this manner for all the data presented here except in a study of the SHG variation over the surface of the film. This is noted in the text. In all cases, a background signal was collected following each SHG measurement by using a blue cut-off filter between the film and the polarization analyzer. The dark counts associated with this measurement constituted less than 10% of the weak SHG signals and were subtracted from the SHG intensity measurement.

The SHG was examined under different incident and reflected polarization combinations, i.e., s,s; s,p;, p,s; and p,p. In these cases a polarization rotator was placed in the laser beam before the film to rotate the polarization from a p incident polarization to an s incident polarization.

The temperature dependent measurements were collected by mounting the films in a Displex cryostat held at 5 x 10^{-6} Torr. The incident laser light was attenuated due to the entrance and exit windows on the cryostat and the effect was compensated for by slightly focussing the beam onto the sample with a 0.5 or 1 meter lens. The polarization combination used was s,p. In this measurement, a Cu vapor laser was used to amplify the CPM and its repetition rate was 6000 Hz. Because of the high repetition rate, a picoammeter was used to detect the output from the PMT.

RESULTS:

Two types of measurements have been collected from the HTSC thin films, the optical measurements related to the SHG signal which are presented here and those which independently characterize the electrical transport and crystallographic structure of the films discussed previously. The optical measurements can be divided into those which test the SHG signal characteristics such as the power dependence, the polarization dependence and rotational anisotropy and those which test different characteristics in the films. These include the SHG, variations over the surface of the films, and the comparison of normal film to oxygen deficient films.

A) Power Dependence

The power dependence of the SHG from a normal YBCO sample was examined. A fit to the equation of $I_{SHG} = I^{n}_{\text{laser power}}$, yields a power dependence of $n = 2.8 \pm 0.2$. To obtain this dependence, the intensity of the SHG was normalized to the reflection of the fundamental

beam from the film surface. Without normalizing to the reflection, the power dependence is much greater than 2.8 indicating that the reflection does not vary linearly with power. This may be do to changes in the optical penetration depth in the film. Because the power dependence from YBCO is somewhat higher than expected, the power dependence from Si(100) was done with the result $n=1.7 \pm .15$. This measurement, taken in the same way, has the value 2 with 90% certainty. We are continuing to investigate the source of the high value from the YBCO film.

B) Polarization Dependence

The intensity of the SHG as a function of the incident and exit polarizations gives some information about the origin of the SHG signal. If the SHG emanates from the surface, it has been shown in some cases that the stronger intensity is with $s_{(out)}$ polarization.[2] Intensity of the $p_{(out)}$ polarization indicates a current flow which is normal to the surface.[3] In the case of a normal YBCO thin film, the most intense SHG is produced in the s,p and p,p configurations. In fact there is a least a factor of 5 lower intensity from the s,s and p,s configurations. To make the comparison between the relative intensity of s,p and p,p polarizations, the incident laser beam was attenuated with the p,p configuration to match the maximum intensity in the s,p configuration. The s,p intensity is 1 ± 0.2 compared to the p,p intensity which is 0.6 ± 0.2. The background or zero values are on the order of 10 cts/s and are about 2% of the s,p intensity in cts/s. Much of the data reported here has been collected with p,p polarization. The exceptions are a few of the diagnostic tests, the film variation test and the temperature dependence.

C) Rotational Anisotropy

Single crystal metals and semiconductors exhibit a variation in the intensity of SHG as the solid state surface is rotated through 360° relative to an incident beam.[13,14] The pattern is related to the point group of the crystalline face. The presence of this characteristic pattern provides direct proof that the SHG signal monitored is generated on the material surface. Rotational anisotropy experiments were performed on Si(111), Si(100) and Si(110) as a test and results similar to those reported by Tom et al.[14] were observed. This was followed by rotational anisotropy experiments on YBCO films deposited on MgO $<100>$. The films have the c-axis perpendicular to the surface and the a and b axis parallel to the surface of the substrate. The a and b axes lengths are 3.856 Å and 3.870 Å, respectively. The in-plane orientation has been determined from XRD pole figure measurements on MGO. The deposited films show maxima at 45° and 90° for a-b misorientations while on $SrTiO_3$ only 90° misorientations are observed. The results of the rotational anisotropy experiment presented here indicate no variation in intensity larger than 15% from these samples, which is on the order of the experimental error.

D) SHG Variation over the Film Surface

The SHG signal was tested in 10 random surface positions on several films. The measurement was made on two normal films (N1 and N6) and two oxygen deficient films (D1 and D6). A bar graph of this variation is shown in Fig 1. The SHG is not normalized to the reflection in this case. The SHG variation at various locations on the film is $\sim 15\%$ for both the normal and oxygen deficient films. We can conclude from this that uniformity of the normal

and oxygen deficient films is similar. Multiple photon events were not counted and so the ratio of the SHG intensity of normal to oxygen deficient films, which is ~ 2.0 from these four films, represents a lower limit of the ratio.

E) SHG from Normal vs. Oxygen Deficient Films

The primary result of this paper is the observation that normal films have a significantly *larger* SHG than oxygen deficient films. Oxygen deficient films have lower T_c's and previous reports have determined a correlation between the T_c and the c-axis parameter.[11,15] As the oxygen stoichiometry decreases from 7 to 6.5, the c-axis lengthens from 11.697 to 11.786 and the T_c decreases from 90° to 55° K.

i) Elastic Backscattering

The oxygen stoichiometry, i.e. 7-δ, from the EBS are given in Table 1. The δ value was estimated from the oxygen atomic fraction. The uncertainty of the EBS measurement is estimated to be ~20%, therefore, the values which are calculated above the theoretical limit of 7.0 are within the estimated uncertainty. The mean value of the oxygen fraction is 7.2 $\pm$ 0.2 from the normal films and it is 6.5 $\pm$ 0.2 from the oxygen deficient films. This confirms that the films designed to be oxygen deficient are indeed that.

ii) Film Parameters

Seventeen samples were tested for linear correlations between the SHG optical measurement and the electronic properties of the films. Approximately half the films were

deposited on MgO <100> and the other half on $SrTiO_3$ <100>. The lattice parameters of $SrTiO_3$ are better matched to the unit cell of the YBCO and may result in better growth characteristics which may be revealed in the SHG intensity from the film. Also, EBS can be used to independently measure the oxygen stoichiometry for films grown on $SrTiO_3$ (but not MgO), providing an independent measure of the oxygen deficiency. However, the $SrTiO_3$ substrate has a strong SHG signal of its own, whereas, the MgO substrate has no SHG signal. For these reasons, both MgO and $SrTiO_3$ films were produced in nearly equal pairs.

Two different film thicknesses were examined; these were ~3000 and ~6000 Å. In addition, the thickness of the substrates (not thought to be important) was also varied between 0.25 and 0.5 mm. These parameters, the x-ray diffraction parameters(c-axis length, δ and the rocking curve widths (Γ)), the electronic properties such as T_c and J_c, along with the SHG intensity and reflection for each film are given in Table 2.

iii) SHG correlations

A linear correlation matrix of the measured parameters is given in Table 3. The two optically determined parameters are the SHG and the reflection parameter. The reflection parameter is simply the laser power which is reflected from the film divided by the incident laser power and is included to account for variation which may exist in the optical quality of each film's surface. First, two separate correlation tables were calculated to compare the films deposited on MgO to those on $SrTiO_3$. No obvious differences were seen, therefore, the two sets were combined for all comparisons shown here.

There are three high correlations shown in Table 3. The highest, -0.92, indicates a negative correlation between the T_c values and the c-axis parameter, which has been previously documented.[11,15] The other two correlations which can be analyzed together, include that of the SHG to T_c which is 0.77 and SHG to c-axis length which is -0.65. If the sample D9 which also has a high rocking curve is not included, these values improve significantly to 0.82 and -0.77, respectively. These are relatively high correlations which link an optical measurement from the surface to the T_c.

Several other conclusions can be drawn from the correlation matrix. Film thickness does not correlate with the SHG. The rocking curve width,(Γ), is somewhat correlated (0.33) to the c-axis parameter which indicates that broader curves are seen with a longer c-axis. The rocking coefficient is not correlated with the SHG (0.18). The reflection measurement is somewhat correlated with the SHG (0.28) and the c-axis parameter (0.30). The correlation of the reflection with Γ (0.60) is due only to Sample D9; this correlation is -0.21 for the other sixteen samples.

iv) Multiple Correlation Analysis

Further statistical analyses were done to determine if multiple correlation would improve the correlation between the SHG and the electronic parameters. These results are shown in Table 4. The first column is the coefficient of multiple (linear) correlation or the R coefficient. It is a correlation value between 0 and 1 which is calculated for the dependent variable labeled

"Y" in column 2 and is correlated with several independent variables labeled "X_n". By examining the R coefficient, we can determine the best combination of variables relevant to the SHG signal. We find a better R coefficient (0.89) when correlating SHG with both reflection and T_c. This is significantly better than the single correlation of SHG with T_c of 0.77 shown in Table 3. The addition of the c-axis parameter and the rocking parameter do not improve the correlation. A plot of the SHG normalized to the reflection factor vs the oxygen content is shown in Fig 2. The oxygen content is calculated directly from the c-axis parameter using the formula given in Ohkubo et al.[11]

v) Plot of SHG as a Function of Oxygen Deficiency, Film thickness and Substrate

Several comparisons are shown in Fig 3 in a plot of SHG intensities related to films characteristics. All the films were normalized to reflection (given in Table 2), the SHG includes multiple photon events and all the films indicate a very large difference in the normal:oxygen deficient film ratio. The comparison labeled "1" are results from the four films, N1, D1, N6 and D6 (from left to right). These 3000 Å films were made about six months prior to the other films in the study. The films labeled "2" have identical (except for age) characteristics to those in "1". These are films N3, D3, N7 and D7. The films labeled "3" are deposited on MgO only (N2, D2 and N5, D5) and compare two 3000 Å films (left) to two 6000 Å films (right). The films in position "4" are four 6000 Å films (N4, D4 and N8, D8) and compare the MgO and $SrTiO_3$ substrates as in comparisons "1" and "2". The collective ratio of the SHG intensity of normal to oxygen deficient films is a factor of ~ 8. These comparisons illustrate that film thickness and the type of substrate are not correlated with the SHG intensity.

F) Temperature Dependence

A decrease in the temperature of the HTSC decreases the volume of the unit cell, providing another way of shortening the c-axis. The temperature dependence of the SHG signal from several normal samples and one oxygen deficient sample was investigated between 300K and 20K to determine if any change in the SHG signal occurs. A plot of the temperature dependence of a normal film is shown in Fig 4. We find a large gradual increase in the SHG from these samples as the temperature is lowered. The temperature dependence of the oxygen deficient sample shows an increase of $\sim 50\%$ compared with increases of about 70% from the normal samples investigated. For comparison, two other materials were tested in the same manner; these were Si(110) (a semiconductor) and a film of gold (a conductor). An increase of about 30% and 15% were seen from the Si(110) and the gold film respectively. The reflection of the fundamental beam intensity was not monitored as a function of temperature during this experiment.

DISCUSSION

i) Is the SHG measurement of the c-axis parameter quantitative?

Using the c-axis dependence on temperature given in Horn et al.,[16] we calculate a correlation of 0.99 of SHG (from the temperature study) with c-axis length. A plot of the Horn et al.[16] data showing the c-axis length varying as a function of temperature is shown with the SHG data in Fig 4. The plots are remarkably similar, showing the same inflection point. An abrupt change in the c-axis parameter has been reported at the T_c by others.[17,18] We do not observe these changes under our experimental conditions.

To determine whether the SHG response to oxygen deficiency and temperature are comparable, we examine the factor by which the SHG increases and compare this to the c-axis change. In the case of temperature as the perturber of the c-axis, a factor of ~ 1.6 is seen in SHG for a change in c-axis of 0.036 (for $300K > T > 100K$). Using Fig 1 data, which most closely resembles the experimental conditions, a factor of ~ 2.4 is seen in SHG (from MgO samples) corresponding to a change in the c-axis of 0.059. These represent comparable ratios, therefore, the SHG intensity is sensitive to changes in the c-axis length caused by either oxygen deficiency or temperature and the magnitude of the SHG appears to be quantitative.

ii) What is the Origin of the SHG Signal?

Previously reported measurements on HTSC thin films have suggested several possible origins of the SHG signal. Because the intensity is relatively high, Akhmanov et al.[4] have suggested that SHG is due to a dipole term and possibly related to the presence of grains in the films. Although XRD indicated the perovskite-like structure, no transport measurements were reported, leaving questions about the composition, phase and structure of the films. Golovashkin et al.[5] suggest that the SHG signals they observe (from bulk $La_{1.8}Sr_{0.2}CuO_4$) may be due to acentric clusters or a breakdown of the inversion symmetry; this is based on a comparison of the SHG intensity compared to a typical ferroelectric, barium titanate. Again, there are questions about the composition and phase of the material used. In the studies reported here the SHG from the superconducting films ($T_c \sim 90$ K) is lower than that of silicon and all the data can be explained assuming a breakdown in the symmetry at the surface and not necessarily from a symmetry breakdown in the bulk material.

A recent optical measurement of radiative properties of YBCO films reports a c-axis parameter dependence and compares these changes to the free electron density calculation.[19] The normal reflectance and normal transmittance are measured at room temperature in the wavelength range from 1 to 100 μm. They illustrate that the reflection data from YBCO with an oxygen content of 7-δ between 7.0 and 6.8 can be modeled using free electron density and an electronic mid-infrared absorption band. For films with lower oxygen content, phonon contributions are included. The magnitude of the reflection change in going from an oxygen content of 7-δ = 7.0 to that of 6.6 is a decrease of $\sim$ 30% with the addition of sharp structural features in the 1 to 100 μm spectral region.

Compression of the c-axis in HTSC's does affect the free electron density of the material.[16] This can be calculated using the equation:

$$n_e = \omega_p^2 \epsilon_o m_e / e^2 \tag{2}$$

where ω_p is the plasma frequency, ϵ_o is the electric permitivity of free space (8.85×10^{-12} $C^2N^{-1}m^{-2}$), m_e is the electron mass (9.110×10^{-31}kg) and e is the electron charge (1.620×10^{-19}C).[19] The free electron density changes in YBCO accompanying oxygen deficiency may explain the SHG intensities presented here. Using the plasma frequencies from Choi et al.,[19] which are 9600 $\pm$ 200 cm^{-1} for 7-δ = 7.0, 4100 $\pm$ 200 cm^{-1} for 7-δ = 6.8 and 4150 cm^{-1} for 7-δ = 6.6, the free electron density is added to Fig. 2 which compares the SHG intensity to c-axis parameter. The scale is arbitrarily chosen to best overlap the SHG data. The flat response of

the SHG in the 6.4 to 6.8 range and the increase in going to 7.0 are consistent with the free electron density.

The predominant SHG intensity comes from the $p_{(out)}$ polarization suggesting that the surface current being probed is perpendicular to the surface plane. We observed weaker signals in the $s_{(out)}$ polarization and under many laser power conditions the $s_{(out)}$ component is on the order of the background noise. A further study of the $s_{(out)}$ and $p_{(out)}$ components may give more information regarding current flow on the surface of the film and perpendicular to the surface. Another diagnostic to obtain further information about the origin of the SHG would be to examine an untwinned, single crystal sample. Further comparisons among different superconducting materials of various free electron densities may prove a connection between the SHG and the free electron density.

iii) Other Possible Sources of SHG

SHG has been demonstrated to be sensitive to a variety of surface structural features including surface roughness and material defects.[20] The effects of optical reflection from different films have been addressed by normalizing to the reflection from each film and no large systematic differences were seen in the reflection of the normal vs the oxygen deficient films. However, it is possible that some surface feature other that free electron density is contributing to or responsible for the SHG. The SHG signal is observed in an evacuated cold finger (5×10^{-6} Torr) at 300 K, however, this does not eliminate the possibility that the SHG is due to monolayers on the surface of the films. UHV studies are needed to see the effect of various

monolayers. In this case the monolayers which adhere to the oxygen deficient films would be different or orient differently than those on normal films.

A number of structural changes in the film could contribute to the SHG signal. They must occur with both oxygen deficiency and temperature variation *or* separate explanations are necessary if a structural change is responsible for the SHG behavior. The range of δ values due to oxygen deficiency used in these experiments is not large enough to result in a phase change in the films. A change from orthorhombic to tetragonal at $\delta \geq 0.6$[21] or 0.7[15] has been demonstrated, however, our values remain $\delta \leq 0.6$ and indicate orthorhombic structure from XRD. Crystallographic structural changes are known to occur due to oxygen deficiency.[8] YBCO films with $\delta=0$ have ordered oxygen vacancies in the basal plane where linear (O-Cu-O) coordination have replaced square planar CuO_4, therefore the δ value can be related to the Cu ion charge.[22] For $\delta=0$, the average copper charge is 2.3, which is a (2:1) mixture of +2 and +3 valence states. There has been conjecture that the large range of mixed valence states in Cu in YBCO may be responsible for its high T_c.[23] When δ is greater than zero, the chains of $(\text{-Cu-O-})_n$ are defective and lead to lattice deformation.[24,25] Large oxygen deficiency has a pronounced effect on both the copper charge state and the nearest-neighbor coordination.[22] Samples with $\delta=0.5$ have an average Cu charge of 2.0.[26]

iv) Is there a Resonance at the Fundamental Wavelength?

One extension of this work would be to change the fundamental wavelength to see the effect of scanning through optical transitions. A resonance between the fundamental wavelength

(or doubled wavelength) and interband transitions or surface states may inhance SHG intensity.[27,28] Resonances with adsorbates on the films may also inhance SHG intensity.[29] There are several reports of a weak transition in the 1.9 to 2.0 eV energy range.[30-32] We have taken absorption spectra which indicate that our samples absorb throughout the visible region between 1.55 eV (800 nm) and 3.1 eV (400 nm) with a broad, small decrease in absorption near 2.0 eV (620 nm). Our spectra of normal and deficient films do not reveal any large differences, however, this does not eliminate the possibility that the normal films may be in resonance and the deficient films not.

CONCLUSIONS

SHG has been used to examine $YBa_2Cu_3O_{7-\delta}$ films as a function of oxygen stoichiometry ($7.0 < 7-\delta < 6.5$) and temperature (300-20 K). A correlation is observed between the c-axis lattice parameter and the SHG intensity. SHG intensity is significantly higher in those films with a compressed c-axis. The SHG intensity correlates well with several electronic transport properties of the films and may be a non-intrusive and non-destructive way of monitoring the free electron density in the HTSC's.

ACKNOWLEDGEMENTS

We thank Dr. D.C. Easter for his assistance in collecting the SHG data, Mr. V. Cestone and Dr. M.E. Reeves for carrying out the magnetic susceptibility characterization, and Dr. R. Gossett for the EBS measurements. Funding for this work was provided by the Office of Naval Research.

TABLE 1

Elastic Backscattering Data

Film ID	Thickness (10^{18}atoms/cm^2)	Calculated Oxygen Content (7-δ)
N6	2.13	7.01
N7	2.71	7.15
N8	5.07	7.33
D6	1.82	6.37
D7	2.55	6.74
D9	1.80	6.52

Film ID	SHG[a]	Subst.	T_c (K)	ΔT[b]	J_c (MA)	X-Ray c-axis (Å)	7-δ[c]	Γ[d]	Reflection[e] (I_{out}/I_{in})	Estimated Film Thickness[f] (Å)	Measured Film Thickness[g] (Å)	Substrate Thickness (mm)
N1	415	MgO	89.6	0.3(S)	3.14	11.691	6.94	.191	0.031	3000		0.50
N2	975	MgO	89.2	0.3(S)	3.4	11.694	6.92	.150	0.046	3000		0.25
N3	772	MgO	89.7	0.4(S)		11.697	6.90	.234	0.044	3000		0.50
N4	458	MgO	89.3	1.7(B)	2.4	11.694	6.92	.230	0.031	6000		0.50
N5	811	MgO	90.7	0.6(S)	2.2	11.697	6.90	.241	0.038	6000		0.25
D1	47	MgO	62.	4.6(B)		11.750	6.56	.231	0.030	3000		0.50
D2	64	MgO	55.	2.8(S)		11.786	6.33	.150	0.049	3000		0.25
D3	123	MgO	69.	3.9(B)		11.751	6.55	.234	0.043	3000		0.50
D4	75	MgO	67.	9.2(B)		11.755	6.53	.274	0.038	6000		0.50
D5	100	MgO	75.	4.6(B)		11.752	6.54	.279	0.039	6000		0.25
N6	313	$SrTiO_3$	91.6	0.5(S)	3.64	11.676	7.03	.150	0.028	3000	2716	0.50
N7	685	$SrTiO_3$	90.5	0.9(S)	2.85	11.690	6.94	.150	0.054	3000	3455	0.50
N8	608	$SrTiO_3$	90.6	0.4(S)	2.0	11.701	6.87	.150	0.049	6000	6465	0.50
D6	77	$SrTiO_3$	65.	3.8(B)		11.726	6.71	.150	0.021	3000	2320	0.50
D7	162	$SrTiO_3$	62.	5.1(B)		11.741	6.62	.167	0.062	3000	3251	0.50
D8	71	$SrTiO_3$	53.	2.8(S)		11.758	6.51	.184	0.055	6000		0.50
D9	706	$SrTiO_3$	72.	1.6(S)		11.760	6.49	.646	0.087	2000	2295	0.50

[a]Collected with p, p polarization.
[b]Broad(B) and sharp(S) transitions are indicated.
[c]Calculated using the c-axis values shown here and 7-δ vs c-axis values from Ref[8].
[d]The rocking curve obtained from XRD. Values at 0.150 represent an experimental limit of XRD.
[e]Ratio of the fundamental beam reflected divided by beam input with p, p polarization.
[f]Estimated from the deposition exposure time.
[g]Obtained from EBS measurement.

TABLE 3

Correlation Matrix of Measured Parameters

	SHG	T_c	c-axis	ΔT	film thickness	subst. thickness	rocking	reflect.
SHG	1							
T_c	.77	1						
c-axis	-.65	-.92	1					
ΔT	-.72	-.68	.66	1				
film thickness	-.10	.07	-.01	.21	1			
subst. thickness	-.18	-.11	.02	.01	-.19	1		
rocking	.18	-.09	.34	.08	-.12	.01	1	
reflect.	.28	-.21	.36	-.08	-.21	.20	.60	1

TABLE 4

Coefficients of Multiple Correlation

R. Coeff.	SHG	Reflection	T_c	c-Axis Parameter	Rocking Curve
0.89	Y	X_1	X_2		
0.85	Y	X_1		X_2	
0.89	Y	X_1	X_2	X_3	
0.89	Y	X_1	X_2	X_3	X_4

REFERENCES

1. Y.R. Shen, Nature, **337**, 519 (1989).

2. Y.R. Shen, The Principles of Non-Linear Optics, Wiley and Sons, NY, p 479-505 (1984)

3. G.L. Richmond, J.M. Robinson, V.L. Shannon, Prog in Surf. Sci., **28**, 1 (1988).

3b S.A. Akhmanov, S.V. Govorkov, N.I.Koroteev, G.I. Petrov, I.L. Shumai, and V.V. Yakovlev, Izvestiya Akademii Nauk SSSR. Seriya Fizicheskaya, **53**, 762-768 (1989).

3c A.I. Golovashkin, V.S. Gorelik, A. M. Agal'tsov, O.M. Ivanenko and K. V. Mitsen, Pis'ma Ah. Eksp.Teor. Fiz, **46**, 155-157 (1989).

4. J.D. Jorgensen, B.W. Veal, W.K. Kwok, G.W. Crabtree, A. Umezawa, L.J. Nowicki and A.P. Paulikas, Phys. Rev. B **36**, 5731-5734 (1987).

5. R.J. Cava, B. Batlogg, C.H. Chen, E.A. Rietman, S.M. Zakurak and D. Werder, Nature (London) **329** 423-425 (1987).

6. R.J. Cava, Science **247**, 656-662 (1990).

6b. S. B. Borisov, I.L. Lyubchanskiĭ, and V.L. Sobolev, Fiz. Tverd. Tela (Leningrad), **31**, 158-162, (1989).

7. D.B. Chrisey, J.S. Horwitz, K.S. Grabowski, M.E. Reeves, M.S. Osofsky, and C.R. Gossett, Proceedings of the Mat. Res. Soc. Fall Mtg (1989).

8. M. Ohkubo, T. Kachi, T. Hioki and J. Kawamoto, App. Phys. Lett. **55** 899-901 (1989).

9. J.H. Claassen, M.E. Reeves and R.J. Soulen, Jr., Rev. Sci Instrum. **62** 992-1004 (1991).

10. D. Guidotti, T.A. Driscoll and H.J. Garritsen, Solid State Comm. **46** 337 (1983).

11. H.W.K. Tom, T.F. Heinz and Y.R. Shen, Phys. Rev. Lett. **51** 1983 (1983).

12. M.E. Parks, A. Navrotsky, K. Mocala, E. Takayama-Muromachi, A. Jacobson and P.K.

Davies, J. Solid State Chem. **79**, 53-62 (1989).

13. P.M. Horn, D.T. Keane, G.A. Held, J.L. Jordan-Sweet, D.L. Kaiser and F. Holtzberg, Phys. Rev. Lett. **59** 2772-2775 (1987).

14. A.I. Golovashkin, O.M. Ivanenko, G.I. Leĭtus, K.V. Mitsen, O.G. Karpinskiĭ and V.F. Shamraĭ, JETP Lett, **46**, 410-412 (1987).

15. R. Srinivasan, K.S. Girirajan, V. Ganesan, V. Radhakrishnan and G.V. Subba Rao, Phys. Rev. B, **38**, 889-892 (1988).

16. B.I. Choi, Z.M. Zhang, M.J. Flik and T. Siegrist, ASME Winter Annual Meeting, Atlanta, GA, Dec 1-6 (1991).

17. S.V. Govorkov, N.I. Koroteev, I.L. Shumay and V.V. Yakovlev, J. Opt. Soc. Am. B, **8** 1023-1027 (1991).

18. E.D. Specht, C.J. Sparks, A.G. Dhere, J. Brynestad, O.B. Cavin, D.M. Kroeger and H.A. Oye, Phys. Rev. B **37**, 7426 (1988).

19. C.P. Poole, Jr., T. Datta, H.A. Farach, "Copper Oxide Superconductors" J. Wiley & Sons, NY, p 109 (1988).

20. P.M. Grant, R.B. Beyers, E.M. Engler, G. Lim, S.S.P. Parkin, M.L. Ramirez, V.Y. Lee, A. Nazzal, J.E. Vazquez and R.J. Savoy, Phys. Rev. B **35** 7242 (1987).

21. J. van den Berg, C.J. van der Beek, P.H. Kes, J.A. Mydosh, G.J. Nieuwenhuys and L.J. de Jongh, Sol. State Comm. **64** 699 (1987).

22. J. van der Berg, C.J. van der Beek, P.H. Kes, G.J. Nieuwenhuys, J.A. Mydosh, H.W. Zandbergen, F.P.F. van Berkel, R. Steens and D.J.W. IJdo, Enrophys. Lett. **4** 737 (1987)

23. R.M. Hazen, L.W. Finger, R.J. Angel, C.T. Prewitt, N.L. Ross, H.K. Mao, C.G. Hadidiacos, P.H. Hor, R.L. Meng and C.W. Chu, Phys. Rev. B **35** 7238 (1987); Erratum. B **36** 3966 (1987).

24. N. Bloembergen and Y.R. Shen, Phys. Rev., **141**, 298 (1966).

25. N. Bloembergen, R.K. Chang and C.H. Lee, Phys. Rev. Lett. **16**, 986 (1966).

26. W. Heuer, L. Schröder, and H. Zacharias, Chem. Phys. Lett. **135**, 299 (1987).

27. S. Tajima, H. Ishii, T. Nakahashi, T. Takagi, S. Uchida, M. Seki, S. Suga, Y. Hidaka, M. Suzuki, T. Murakami, K. Oka and H. Unoki, J. Opt. Soc. Am. B **6** 475-482 (1989).

28. M. Garriga, J. Humlíček, J. Barth, R.L. Johnson and M. Cardona, J. Opt. Soc. Am. B **6** 470-474 (1989).

29. I. Fugol, G. Saemann-Ischenko, V. Samovarov, Y. Rybalko, V. Zhuravlev, Y. Ströbel, B. Holzäpfel and P. Berberich, Solid State Comm. **80** 201-206 (1991).

FIGURE CAPTIONS

Fig. 1 SHG intensity in cts/s for the films N1 (Normal/MgO), D1 (Ox.Def./MgO), N6 (Normal/$SrTiO_3$) and D6 (Ox.Def./$SrTiO_3$) taken at 10 different positions on the film. The SHG variation at each film position represents the error in the measurement plus any variation in the film surface. The effect of oxygen deficiency is much larger than these errors combined.

Fig. 2 The SHG intensity/reflection vs the oxygen content of the 17 films in the study. Also shown are the free electron number densities at various oxygen stoichiometries taken from Ref. 16. These are arbitrarily scaled to the SHG data points.

Fig. 3 SHG intensities from sixteen films are shown. (1) Films which are normal and oxygen deficient on MgO and $SrTiO_3$, all 3000 Å thick, made 6 months prior to test. (2) Identical to #1, however, made a few weeks prior to test. (3) Films on Mgo only 3000 Å (two left) compared to 6000 Å (two right) of same age as #2. (4) Films 6000 Å thick with of same age as #2 and #3. See text for film identification.

Fig. 4 SHG intensity as a function of film temperature. (o) The film shown is normal on MgO, 400 Å thick. Also shown is the c-axis compression as a function of temperature (-) from Ref. 13.

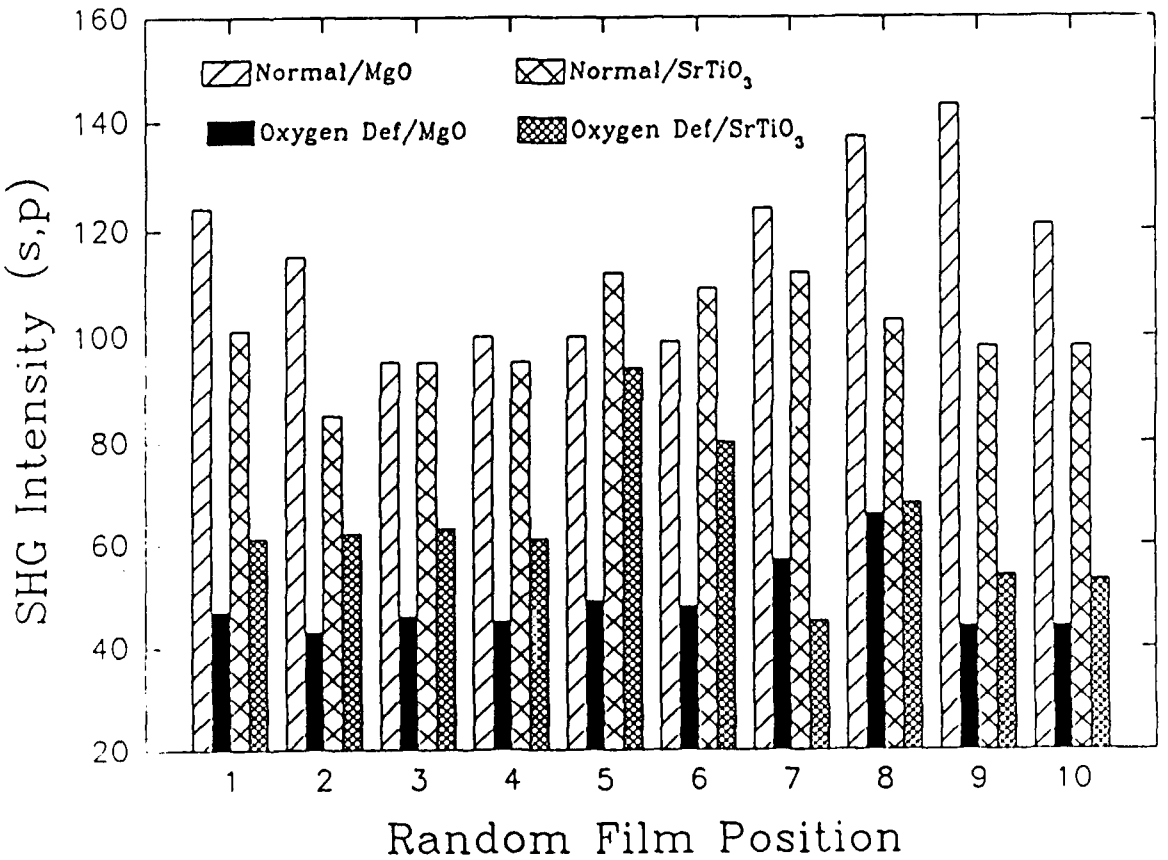
160
140
120
100
80
60
40
20
SHG Intensity (s,p)
Normal/MgO
Normal/SrTiO3
Oxygen Def/MgO
Oxygen Def/SrTiO3
1
2
3
4
5
6
7
8
9
10
Random Film Position

Fig 1

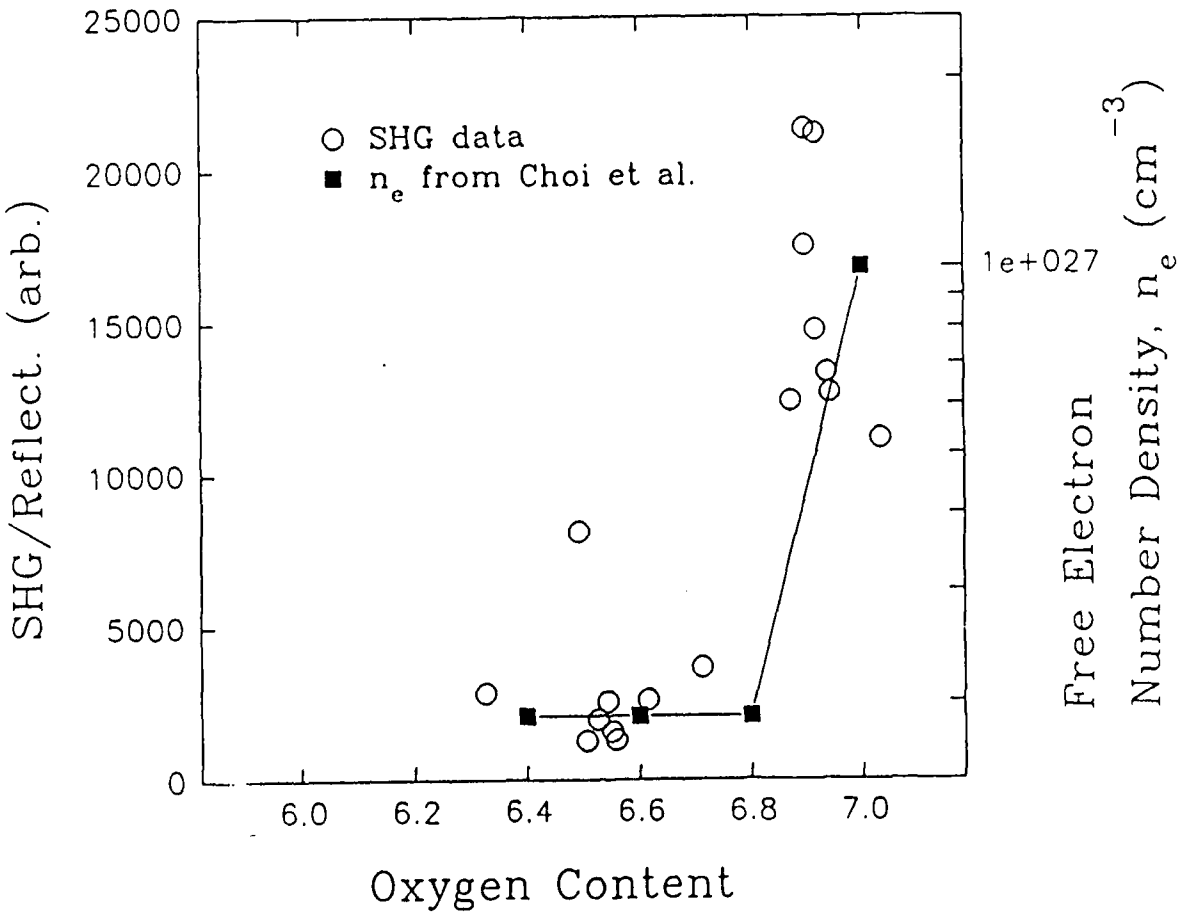
25000
20000
15000
10000
5000
0
SHG/Reflect. (arb.)
SHG data
n_e from Choi et al.
1e+027
Free Electron
Number Density, n_e (cm^{-3})
6.0
6.2
6.4
6.6
6.8
7.0
Oxygen Content

Fig 2

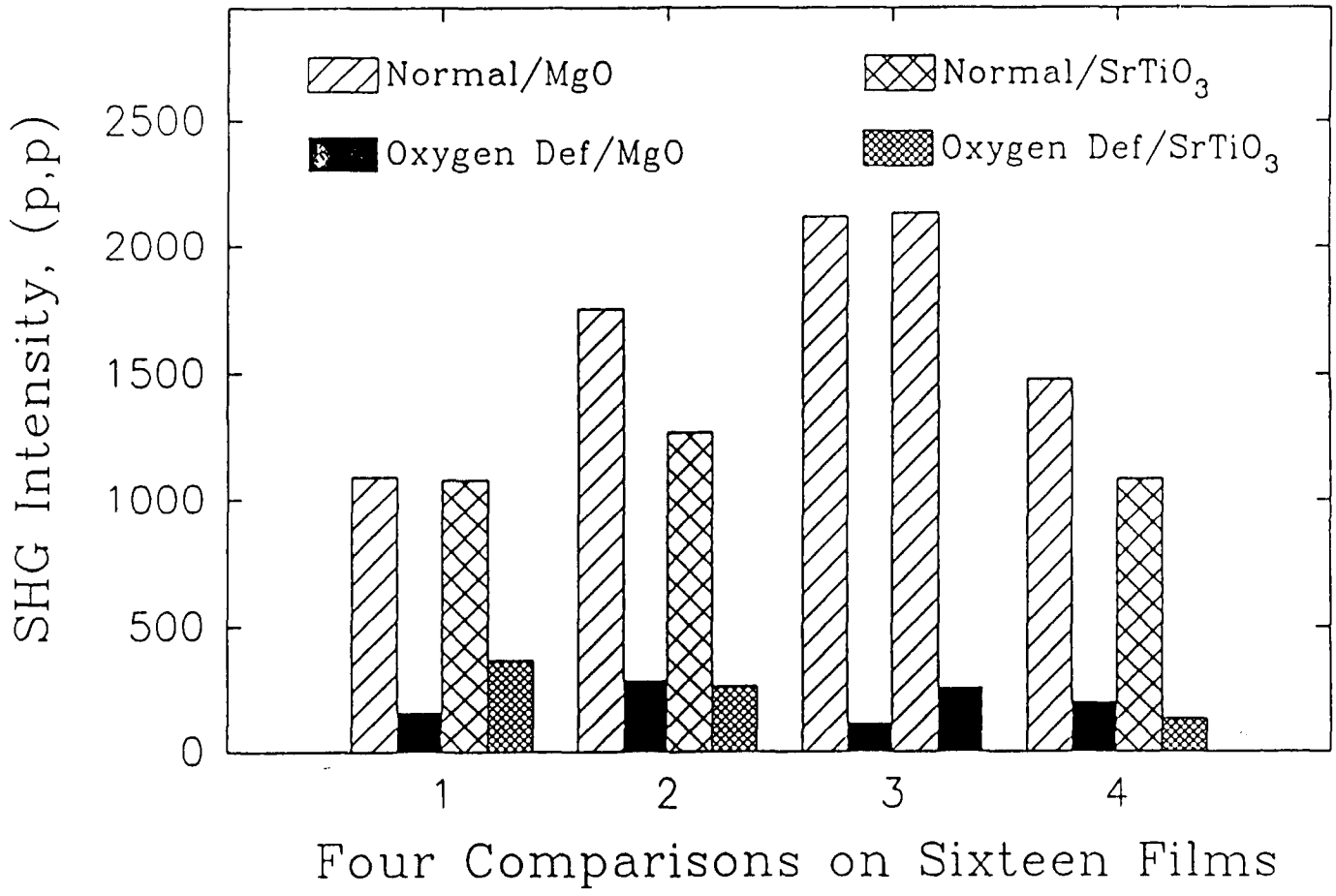
Normal/MgO
Normal/SrTiO3
Oxygen Def/MgO
Oxygen Def/SrTiO3
SHG Intensity, (p,p)
2500
2000
1500
1000
500
0
1
2
3
4
Four Comparisons on Sixteen Films

Fig 3

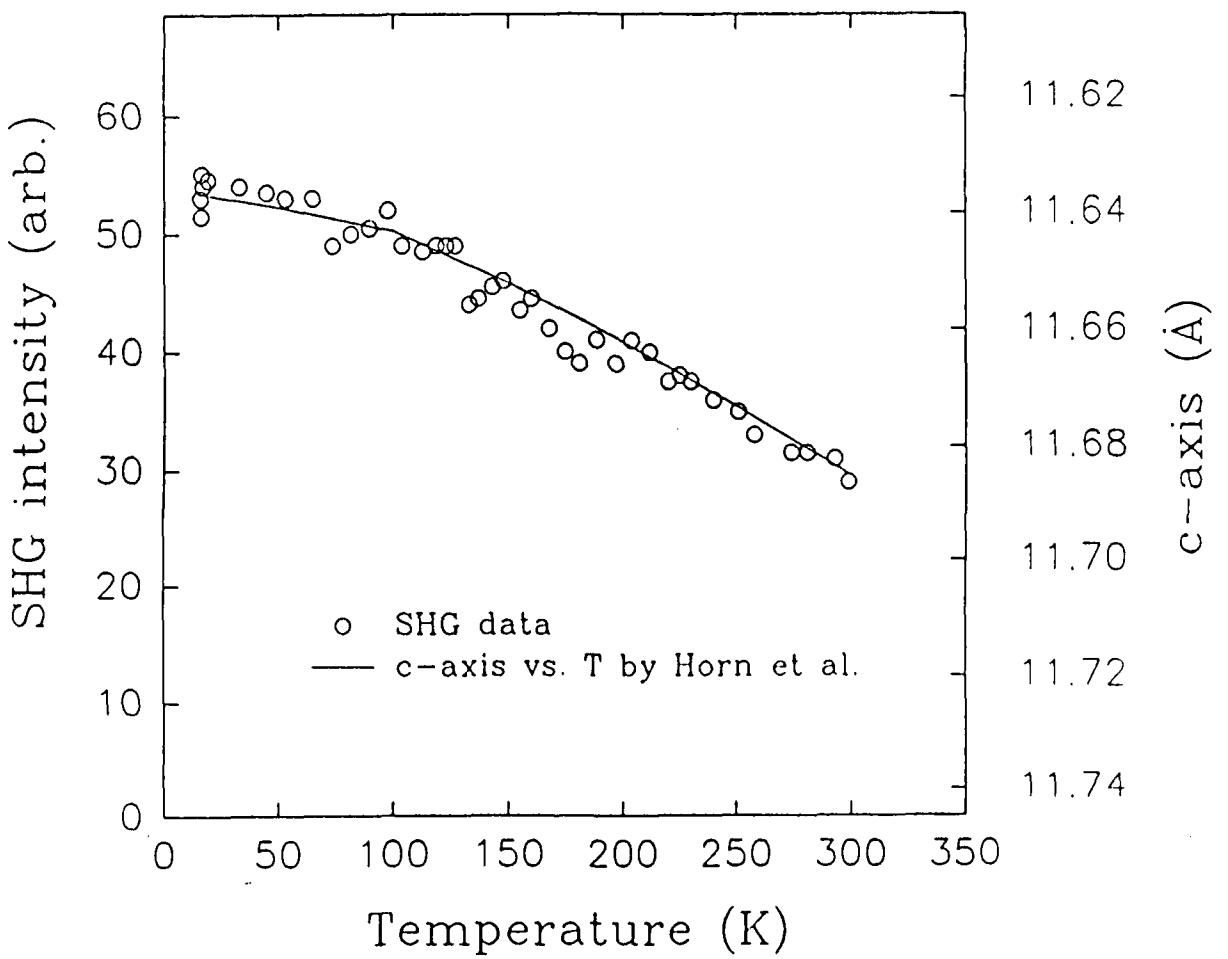
SHG intensity (arb.)
60
50
40
30
20
10
0
0
50
100
150
200
250
300
350
Temperature (K)
11.62
11.64
11.66
11.68
11.70
11.72
11.74
c-axis (Å)
SHG data
c-axis vs. T by Horn et al.

Fig 4

SHG-T-C

TECHNICAL REPORT DISTRIBUTION LIST - GENERAL

Office of Naval Research (2)
Chemistry Division, Code 1113
800 North Quincy Street
Arlington, VA 22217-5000

Dr. James S. Murday (1)
Chemistry Division, Code 6100
Naval Research Laboratory
Washington, DC 20375-5000

Dr. Robert Green, Director (1)
Chemistry Division, Code 385
Naval Air Weapons Center
Weapons Division
China Lake, CA 93555-6001

Dr. Elek Lindner (1)
Naval Command, Control and Ocean
Surveillance Center
RDT&E Division
San Diego, CA 92152-5000

Dr. Bernard E. Douda (1)
Crane Division
Naval Surface Warfare Center
Crane, IN 47522-5000

Dr. Richard W. Drisko (1)
Naval Civil Engineering
Laboratory
Code L52
Port Hueneme, CA 93043

Dr. Harold H. Singerman (1)
Naval Surface Warfare Center
Carderock Division Detachment
Annapolis, MD 21402-1198

Dr. Eugene C. Fischer (1)
Code 2840
Naval Surface Warfare Center
Carderock Division Detachment
Annapolis, MD 21402-1198

Defense Technical Information (2)
Center
Building 5, Cameron Station
Alexandria, VA 22314